0026-895X/02/6202-423–431$7.00
MOLECULAR PHARMACOLOGY
Vol. 62, No. 2
1693/1000028
Mol Pharmacol 62:423–431, 2002
Printed in U.S.A.

Inflammation Modulates the Interaction of Heterogeneous Nuclear Ribonucleoprotein (hnRNP) I/Polypyrimidine Tract Binding Protein and hnRNP L with the 3′Untranslated Region of the Murine Inducible Nitric-Oxide Synthase mRNA

MALIN SÖDERBERG, FRANÇOISE RAFFALLI-MATHIEU, and MATTI A. LANG

Division of Biochemistry, Department of Pharmaceutical Biosciences, Uppsala University, Uppsala, Sweden

Received February 22, 2002; accepted April 30, 2002

This article is available online at http://molpharm.aspetjournals.org

ABSTRACT

Interaction of two members of the heterogeneous nuclear ribonucleoprotein (hnRNP) family with the 3′untranslated region (UTR) of the murine inducible nitric-oxide synthase (iNOS) mRNA is demonstrated in this study. An iNOS RNA-protein complex is formed using protein extracts from untreated and septic shock treated mouse liver. UV cross-linking reveals that the complex consists of at least two proteins, with apparent molecular masses of 60 and 70 kDa, respectively. The 60-kDa protein binding site lies within a 112-nt pyrimidine-rich sequence, approximately 160 nt from the coding sequence, and the RNA-protein complex can be precipitated by a monoclonal antibody directed against hnRNP I [also named polypyrimidine tract binding protein (PTB)]. The 70-kDa protein binds a 43-nt sequence near the 3′end of the 3′UTR and is immunoprecipitated by a monoclonal antibody against hnRNP L. A computer-simulated conformation of the 3′UTR suggests that both binding sites reside in regions easily accessible for a protein. Supershifts of the native RNA-protein complex could only be achieved with anti-hnRNP L, suggesting that within this multiprotein RNA complex, only hnRNP L is exposed to the antibodies, whereas the hnRNP I/PTB is mainly responsible for its interaction with the mRNA. Up-regulation of iNOS by septic shock reduces the RNA-protein complex formation, thus showing that hnRNP I/PTB and hnRNP L binding to the iNOS mRNA is modulated by inflammation. This suggests a novel function for the two previously described proteins as regulators of the *iNOS* gene.

The inducible nitric-oxide synthase (iNOS) is up-regulated by immunologic and inflammatory stimuli, such as lipopolysaccharides (LPS) or cytokines, resulting in increased production of nitric oxide (NO) (for review, see Rao, 2000). Induction of iNOS is part of the antimicrobial and tumoricidal actions of macrophages (Nathan and Hibbs, 1991; Cui et al., 1994) but may also have detrimental effects, such as tissue damage observed in, for example, arthritis, type I diabetes, and septic shock (Corbett and McDaniel, 1992; McCartney-Francis et al., 1993; Morikawa et al., 1999). The diversity of NO effects implies a tight regulation of its production.

Research to date has shown that regulation of the *iNOS* gene is complex, implicating transcriptional, post-transcriptional/translational, and post-translational mechanisms (Geller and Billiar, 1998), and several consensus sequences and corresponding *trans*-acting factors contributing to the transcriptional control of both the human and murine *iNOS* genes have been described previously (Lowenstein et al., 1993; Xie et al., 1993; de Vera et al., 1996; Chu et al., 1998).

Compared with its transcriptional control, the post-transcriptional regulation of the *iNOS* gene is poorly understood yet probably an important part of the overall regulation. For example, in mouse peritoneal macrophages, transforming growth factor β1 suppresses iNOS expression by decreasing iNOS mRNA stability and translational efficiency and by increasing the degradation of iNOS protein (Vodovotz et al., 1993). On the other hand, iNOS mRNA stability has been shown to increase during induction of iNOS expression (Weisz et al., 1994). In none of the cases, however, are the mechanisms behind the events known. The 3′untranslated region (UTR) of both human and murine iNOS contains conserved AU-rich sequences, known to mediate mRNA instability in many labile cytokine and proto-oncogene transcripts (Evans et al., 1994; Ross, 1995). Whether these AU-rich sequences play a role in the iNOS mRNA stability remains unknown (Geller and Billiar, 1998). In one report, Rodriguez-Pascual et al. (2000) show the binding of the *Drosophila melanogaster* ELAV (embryonic lethal abnormal vision)-like

ABBREVIATIONS: iNOS, inducible nitric oxide synthase; LPS, lipopolysaccharide; NO, nitric oxide; UTR, untranslated region; hnRNP, heterogeneous nuclear ribonucleoprotein; PTB, polypyrimidine tract binding protein; DTT, dithiothreitol; GAPDH, glyceraldehyde-3-phosphate-dehydrogenase; PCR, polymerase chain reaction; nt, nucleotide(s); PAGE, polyacrylamide gel electrophoresis; CS, coding sequence.

TABLE 1
Primers used for PCR
The different sets of primers used to amplify various fragments from iNOS coding sequence and 3′UTR are shown, as seen in Figure 2. T7 represents the T7 RNA polymerase promoter sequence 5′-TAATACGACTCACTATAGGGAGA-3′. The nucleotide assignments correspond to the iNOS sequence in GenBank reference number M92649 (Lowenstein et al, 1992).

Primer	Orientation	Oligonucleotide Sequence (5′-3′)	nt Assignment
P1	Sense	T7-AGGCTCTGACAGCCCAGAGTT	3618–3638
P2[a]	Antisense	CGAATTGGAGCTCCACCGC	11–29
P3	Sense	T7-GTGTCTGCAGCACTTGGATC	2998–3017
P4	Antisense	ACTCAGTGCCAGAAGCTGGA	3638–3657
P5	Sense	T7-ACAGCCCAGAGTTCCAGCT	3626–3644
P6	Antisense	GGAGAGAGATTTAGTAGTCCAC	3762–3783
P7	Sense	T7-GTGGACTACTAAATCTCTCT	3762–3781
P8	Antisense	CTGTACATAGTGCAGCTAA	3961–3979
P9	Sense	T7-ATACTTAGCTGCACTATGTACAG	3957–3979
P10	Sense	T7-TTGGAGCTGAGAGCAGAG	3874–3891
P11	Antisense	CTGTACATAGTGCAGCTAAG	3960–3979
P12	Antisense	ATTGGGAGTAGACAAAAGTATCT	4007–4029
P13	Sense	T7-GATGGCTTGGGCCTTTCCT	4030–4048
P14	Sense	T7-AATATTTATATAAAATACA	4068–4086

P, Primer; nt, nucleotide.
[a] P2 is within the pBluescript multiple cloning site flanking the cloned iNOS cDNA (in the *Not*I site). All fragments produced with P2 were digested with *Not*I to remove the additional 29 nt.

protein HuR to AU-rich motifs in the 3′UTR of human iNOS mRNA and speculate that it could mediate the post-transcriptional events during the cytokine-induced expression of the human iNOS.

In the present study, we analyze the interaction of cytoplasmic liver proteins with the murine iNOS mRNA. We demonstrate that inflammation affects the interaction of a multiprotein complex formation with the 3′UTR of the iNOS mRNA. The proteins in the complex seem to be heterogeneous nuclear ribonucleoprotein I (hnRNP I) (also named polypyrimidine tract binding protein, PTB) and hnRNP L, and they bind at two distinct regions of the 3′UTR, both easily accessible for *trans*-acting factors. The possible novel functions of hnRNP I/PTB and hnRNP L as regulators of the iNOS expression are discussed.

Materials and Methods

Reagents. D-Galactosamine was from ICN Pharmaceuticals (Costa Mesa, CA), RNase A from Roche Diagnostics Scandinavia (Bromma, Sweden), RNase T1 from Invitrogen AB (Lidingö, Sweden), Amplitaq Gold and dNTP mix from PerkinElmer Life Sciences (Boston, MA), and T7 RNA polymerase from Promega (Madison, WI). Isotopes ([α-^{32}P]UTP and [α-^{32}P]dCTP) were from Amersham Biosciences (Piscataway, NJ). Protease inhibitors (phenylmethylsulfonyl fluoride, leupeptine and DTT), yeast tRNA, lipopolysaccharide (*Escherichia coli*, serotype 0127:B8), and homoribopolymers [poly(A), poly(U), poly(C) and poly(G)] were from Sigma-Aldrich Sweden AB (Stockholm, Sweden).

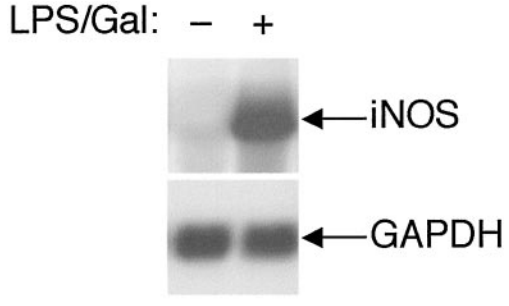

Fig. 1. iNOS mRNA induction. Liver RNA (20 μg) prepared from mice (~25g), untreated (−) or "septic shock"-treated (LPS/Gal) (+) i.p. with LPS (100 ng) and D-galactosamine (10 mg) for 6 h, were used for Northern blot analysis. Control animals received saline vehicle only. Hybridization was performed with 1.7×10^6 cpm of radiolabeled iNOS 4-kilobase cDNA fragment. GAPDH mRNA levels are shown as controls for RNA loading.

Antibodies and Oligodeoxyribonucleotides. Monoclonal antibodies 4D11 (anti-hnRNP L) and 4F4 (anti-hnRNP C) were generously provided by Dr. Gideon Dreyfuss (Howard Hughes Medical Institute, University of Pennsylvania, Philadelphia, PA). Anti-hnRNP I/PTB was purchased from Zymed Laboratories (South San Francisco, CA). All of the oligodeoxyribonucleotides used in the study were from Sigma Genosys (Pampisford, Cambridgeshire, UK).

Animals. Male DBA/2J mice, 6 to 10 weeks old, were provided by Möllegaard (Ejby, Denmark). The mice were kept at the animal facility at the Biomedical Centre in Uppsala and fed chow and water *ad libitum*. They were allowed to acclimatize for 1 week before treatment. The mice (~25 g) were treated intraperitoneally with 100 ng of LPS and 10 mg of D-galactosamine dissolved in saline. Control mice received saline only. After 6 h of treatment, the animals were sacrificed and livers were removed. The studies were approved by the Ethical Committee in Uppsala (Sweden) with approval number C3/1 and performed accordingly.

RNA Isolation and Northern Blot Analysis. Total RNA was isolated from the liver samples using an RNeasy Midi kit (QIAGEN GmbH, Hilden, Germany) according to the manufacturer's protocol. Total RNA (20 μg) was subjected to electrophoresis in 1.2% agarose/formaldehyde gel, transferred to a Hybond-N nylon membrane (Amersham Biosciences AB, Uppsala, Sweden) and UV cross-linked before hybridization. The 4-kilobase *Not*I fragment, excised from a plasmid containing the murine iNOS cDNA (kindly provided by Dr. Charles J. Lowenstein, John Hopkins University, Baltimore, MD), was radiolabeled with [α-^{32}P]dCTP using the Megaprime labeling kit (Amersham Biosciences AB). Unincorporated nucleotides were removed by using a G-50 column (Amersham Biosciences AB). Both prehybridization and hybridization were performed at 65°C in Church buffer (Church and Gilbert, 1984) modified to contain 0.25 M $NaHPO_4$, pH 7.2, 7% SDS, and 1 mM EDTA. Hybridization was performed overnight with 1.7×10^7 cpm of radiolabeled probe. To assess equal loading of the samples, the mRNA level of the housekeeping gene glyceraldehyde-3-phosphate-dehydrogenase (*GAPDH*) was measured using the radiolabeled GAPDH cDNA (BD Clontech, Palo Alto, CA).

Preparation of Liver Cytoplasmic Extracts. For preparation of the crude cytoplasmic protein extracts, excised mouse liver was homogenized in 15 mM HEPES buffer, pH 7.6, containing 3 mM $MgCl_2$, 40 mM KCl, 1 mM DTT, 0.5 mM phenylmethylsulfonyl fluoride, 10 ng/μl leupeptine, and 0.4% igepal. The homogenate was

centrifuged at 12,000*g* for 10 min at 4°C. The supernatant, corresponding to the cytoplasmic extract, was aliquoted and stored at −80°C until further use. Protein concentration was measured by the method of Lowry et al. (1951).

In Vitro Transcription. Using different sets of primers, cDNAs encoding various subfragments of murine iNOS 3′UTR and coding sequence (see Fig. 2, Table 1) were obtained by PCR using the iNOS-containing plasmid as a template. All PCR reactions were performed with *Taq* DNA polymerase. After 10 min at 95°C followed 30 cycles: 94°C, 1 min; 52°C, 1 min; 72°C, 1 min. The nucleotide positions of the primers refer to the cDNA map as published by Lowenstein et al. (1992). Primer 2 hybridizes to the pBluescript plasmid, 29 nt downstream of the *Not*I cloning site. All fragments produced with primer 2 were further subjected to cleavage with *Not*I to eliminate the plasmid sequence. Sense oligonucleotides contained 23 nt corresponding to the T7 RNA polymerase promoter. PCR-amplified products were transcribed with T7 RNA polymerase in the presence of [α-^{32}P]UTP (800 Ci/mmol) using standard protocols (Promega). The 218- and 81-nt fragments were cut with the restriction enzymes *Ear*I and *Ssp*I before use as templates for *in vitro* transcription, to generate the resulting 112- and 41-nt probes, respectively. Unincorporated nucleotides were removed by using a G-50 column (Amersham Biosciences AB). Unlabeled RNA competitors were transcribed under similar conditions, with the radiolabeled nucleotide substituted with 0.5 mM UTP.

UV Cross-Linking. Binding reactions were carried out for 12 min at room temperature using 200,000 cpm of ^{32}P-labeled RNA transcript and 25 μg of protein extracts, in a total volume of 20 μl containing 10 mM HEPES, pH 7.6, with 3 mM $MgCl_2$, 40 mM KCl, 5% glycerol, 1 mM DTT, and 1 μg of yeast tRNA. The reaction mixture was then placed on ice and exposed to UV light for 20 min in a Spectrolinker XL-1000 UV cross-linker (Spectronics, Westbury, NY). Subsequently, unbound RNA was digested with 2 μg of RNase A at 37°C for 20 min. The samples were denatured under nonreducing conditions and separated by SDS/PAGE (12%). Finally, the gel was dried and autoradiographed overnight. For competition experiments, the protein extract was preincubated for 5 or 10 min with the indicated unlabeled competitors.

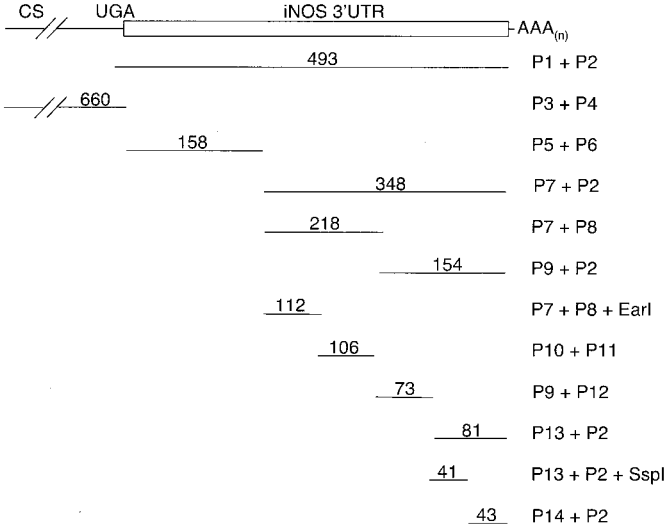

Fig. 2. iNOS mRNA fragments used for RNA-protein interaction analysis. The schematic of the iNOS 3′UTR, part of the coding sequence (CS) and the individual transcripts used in the RNA binding studies are shown. The oligonucleotides used for amplification in the PCR reactions are indicated on the right; see Table 1 for details of the oligonucleotides used. The number of nucleotides for each probe is indicated. P2 is an oligonucleotide located in the plasmid sequence where iNOS cDNA is cloned. All transcripts generated with P2 were therefore cut with *Not*I after PCR amplification, to remove the 29-nt plasmid sequence. The 218- and 81-nt templates were cut with the restriction enzymes *Ear*I and *Ssp*I, before in vitro transcription, to generate the 112- and 41-nt probes, respectively.

Immunoprecipitation. The UV cross-linked complexes were immunoprecipitated essentially as described by Hamilton et al. (1993). A typical UV cross-linking was performed with 40 μg of liver cytoplasmic extract and 200,000 cpm of radiolabeled 112- or 81-nt probes, respectively. After RNase A digestion, the RNA-protein complexes were incubated with a 1:500 dilution of anti-hnRNP L (4D11), anti-hnRNP I/PTB, or anti-hnRNP C (4F4) (used as a control antibody) monoclonal antibodies for 2h at 4°C. The samples were then incubated with 30 μl of protein A-Sepharose beads (Amersham Biosciences AB) for 1 h at 4°C. The beads were recovered by brief centrifugation and washed three times in PBS. The proteins were denatured and analyzed by SDS/PAGE (12%). After drying, the gels were exposed to X-ray films.

RNA Mobility Shift Assay and Supershift Assay. Binding conditions were the same as described above, using 5 or 25 μg of liver cytoplasmic extract, as indicated. After binding, the reaction mixtures were treated with RNase T1 (20 units) for 20 min at room temperature. The RNA-protein complexes were resolved on nondenaturing 7% polyacrylamide gels (acrylamide/bisacrylamide ratio, 37.5:1) with 50 mM Tris/glycine, pH 8.8, as running buffer. The gels were dried and visualized by autoradiography. For competition experiments, unlabeled competitors were added 10 min before the addition of the radiolabeled RNA. In supershift assays, 5 μg of protein extract was incubated with the RNA probe as described above. After RNase T1 treatment, 1 μl of anti-hnRNP L (4D11) anti-hnRNP I/PTB or anti-hnRNP C (4F4) monoclonal antibodies, respectively, were added to the mixtures and incubated for another 10 min, before loading on a native gel, as described by Min et al. (1995). In several cases, lanes of one or several gels from the same UV cross-linking or RNA mobility shift experiment with identical exposure times, have been combined into one figure.

Computer Analysis. The Mfold program was used to perform computer secondary structure predictions of the iNOS 3′UTR sequence (Mathews et al., 1999; Zuker et al., 1999).

Results

Demonstration of High-Affinity Protein Binding to the 3′UTR of the Murine iNOS mRNA, and Dependence of the RNA-Protein Complex Formation on Septic Shock. Mice treated with LPS and D-galactosamine develop septic shock (Barton and Jackson, 1993), a condition that induces the *iNOS* gene (Morikawa et al., 1999). This was used to mimic an infection and to achieve up-regulation of iNOS mRNA. As expected, an increase of iNOS mRNA was seen after 6 h of treatment (Fig. 1).

Evidence suggests that iNOS induction involves post-transcriptional control of both the murine and human genes (Vodovotz et al., 1993; Weisz et al., 1994; Rodriguez-Pascual et al., 2000). To screen for possible *trans*-acting factors interacting with the 3′UTR of the murine iNOS mRNA, binding reactions were performed with the entire 3′UTR as a probe (see Fig. 2 and Table 1) and liver cytoplasmic protein extracts from septic shock-treated and -untreated animals. As shown in Fig. 3, at least two retarded bands could be seen in a gel mobility shift assay. Complex I (▷) shows the highest intensity with control extracts, disappearing almost entirely upon LPS-galactosamine treatment, whereas complex II (▶) has the highest intensity after the septic shock (Fig. 3). In repeated experiments, the disappearance of complex I upon LPS-galactosamine treatment was reproducible.

To determine the apparent molecular masses of the proteins interacting with the iNOS 3′UTR, we performed UV

cross-linking experiments. Two complexes with apparent molecular masses of 60 and 70 kDa were resolved (Fig. 4). In accordance with the gel shift assay, the intensity of the complexes, in particular that of the 60-kDa complex, decreases by septic shock. Proteinase K treatment of the reaction mixture prevented the complex formation, demonstrating that the binding factors are proteins (data not shown).

To examine the specificity of the RNA-protein interactions, we performed competition experiments. The complex formation with iNOS 3′UTR and cytoplasmic extracts from untreated animals could be inhibited by unlabeled iNOS 3′UTR as a competitor (Fig. 5A), but not by tRNA or a 660 nt fragment of the iNOS coding sequence (Fig. 5A). High concentrations of tRNA, however, reduced the complex formation. This shows a high-affinity binding of the native complex to iNOS 3′UTR. In support of this, competition experiments with UV cross-linking showed an efficient inhibition of both the 60- and 70-kDa complex formations by the unlabeled iNOS 3′UTR probe. In contrast, a much weaker inhibition was observed by the other competitors (Fig. 5b). The 70-kDa complex was more susceptible to tRNA competition than the 60-kDa complex, and was also slightly affected by the unlabeled coding sequence, reflecting differences in affinities of the two proteins to the iNOS mRNA. We also performed gel shift competition experiments with unlabeled homoribopolymers, resulting in an efficient inhibition by poly(U), and less by poly(C), poly(G), and poly(A), respectively (data not shown). This indicates that one (or several) of the proteins in the iNOS 3′UTR complex has a strong affinity for U-rich sequences.

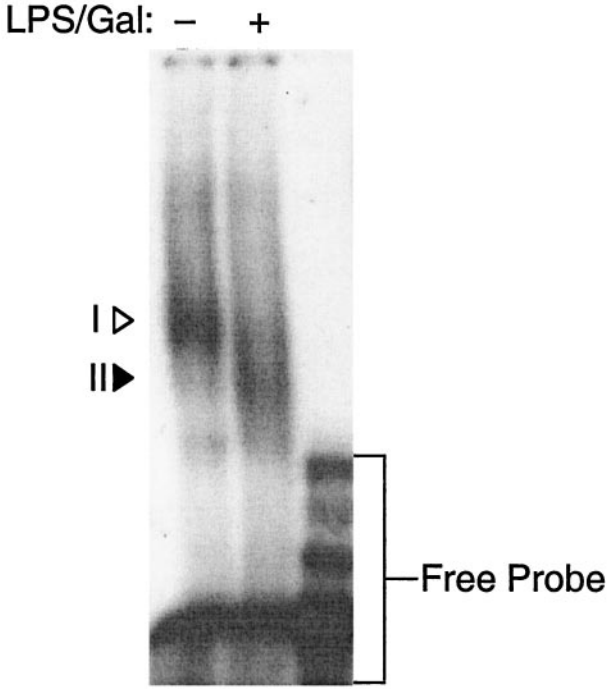

Fig. 3. Protein complex formation with the iNOS 3′UTR is sensitive to septic shock treatment. RNA gel mobility shift assay with ^{32}P-radiolabeled iNOS 3′UTR RNA full-length probe (493 nt; see Fig. 2) incubated with 25 μg of cytoplasmic protein extract from mice untreated (–) or treated (+) with LPS (100 ng) and D-galactosamine (10 mg) for 6 h. Control animals received saline vehicle only. The third lane contains no extract. The positions of the free RNA probe and the RNA-protein complexes I (▷) and II (▶) are indicated.

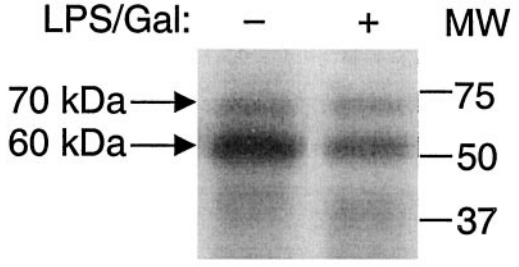

Fig. 4. Determination of the apparent molecular masses of the proteins binding to the iNOS 3′UTR mRNA. iNOS 3′UTR full-length RNA probe was incubated with 25 μg of cytoplasmic protein extract from untreated (−) or "septic shock"-treated (LPS/Gal) (+) mice, UV cross-linked, and resolved on SDS/PAGE (12%) as described under *Materials and Methods*. Molecular mass (MW) standards in kilodaltons are indicated on the right. The 70- and 60-kDa complexes are marked with arrows.

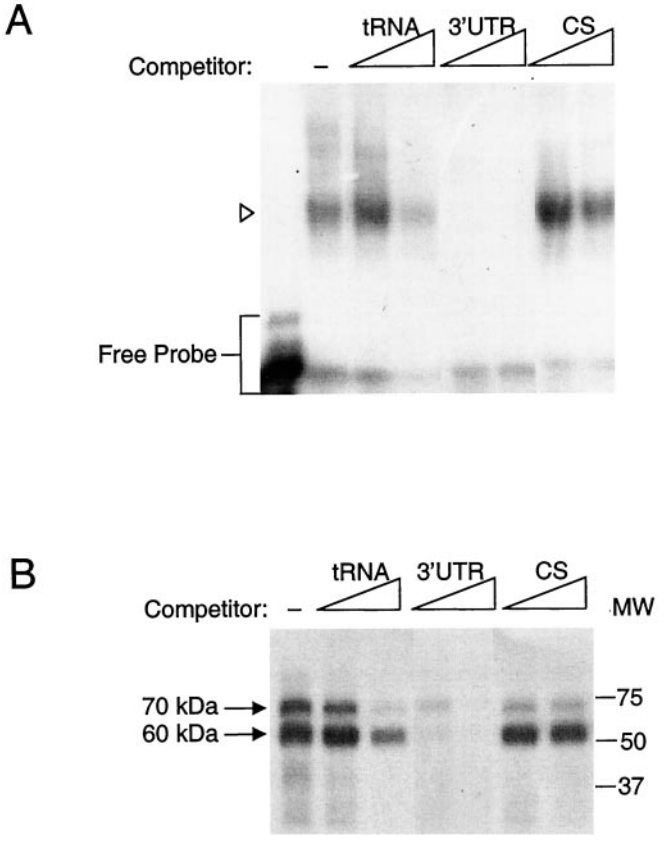

Fig. 5. Specificity of the RNA-protein complex formation. A, RNA gel mobility shift assay was carried out with the ^{32}P-radiolabeled iNOS 3′UTR RNA full-length probe (493 nt) incubated without extract in the first lane (free RNA probe) or with 25 μg of protein extract from untreated animals in the absence (−) or presence of 1 or 5 μg of unlabeled yeast tRNA; 0.5 or 1 μg of unlabeled iNOS 3′UTR RNA probe, or with 0.5 or 1 μg of unlabeled iNOS coding sequence (CS) RNA probe (660 nt) as shown. The unlabeled competitor was added 10 min before the radioactive probe. Complex I is shown. B, UV cross-linking assay with the ^{32}P-radiolabeled iNOS 3′UTR RNA full-length probe (493 nt) and 25 μg of cytoplasmic protein extract from untreated mice, incubated in the absence (−) or presence of 1 or 5 μg of unlabeled yeast tRNA; 135 or 300 molar excess of unlabeled iNOS 3′UTR RNA probe, or with 135 or 300 molar excess of unlabeled iNOS coding sequence (CS) RNA probe, as indicated. The 60- and 70-kDa complexes are shown. The unlabeled competitor was incubated for 10 min with the protein extract before addition of the radiolabeled probe. Molecular mass (MW) standards in kilodaltons are indicated on the right.

Mapping of the Binding Regions for Proteins Involved in the 60- and 70-kDa Complexes. The strategy for mapping the protein binding sites at the iNOS 3′UTR is shown in Fig. 2 and Table 1. A total of 11 RNA probes were prepared and used in both gel mobility shift and UV cross-linking analyses. RNA probes of 158 and 348 nt, respectively, were first created from two sections of the iNOS 3′UTR sequence, as shown in Fig. 2. We detected the gel-shifted complex, resembling the native complex, only with the longer probe, as shown in Fig. 6A. Using smaller probes, the same complex was seen with the 218-nt sequence, whereas the 154-nt probe gave a higher complex also sensitive to septic shock (Fig. 6A). With the 112-nt probe, we still obtained a complex similar to that seen with the 3′UTR probe, whereas the 81-nt probe showed a profile partly similar to the 154-nt probe (Fig. 6a). It is noteworthy that with both the 348-, 218-, and 112-nt probes, the sensitivity of complex formation to septic shock, is conserved.

To search for the binding sites of the 60- and 70-kDa proteins, UV cross-linking with the relevant probes was performed. As seen in Fig. 6B, both protein complexes appear with the 348-nt probe, whereas only one of the two binds the 218 and 154-nt probes, respectively (Fig. 6b). The binding site of the 60-kDa protein was located to the 112-nt probe, ~160 nt from the coding region, and that of the 70-kDa protein to the 81-nt sequence at the 3′end of the 3′UTR, as shown in Fig. 6B. Further division of the 81-nt sequence revealed a weak complex with the 41-nt probe and a stronger one with the 43-nt sequence, possibly containing the primary binding site for the 70-kDa protein (Fig. 6B).

The primary binding sites for the two proteins were defined by using antisense oligonucleotides covering different regions of the 112- (AS1-AS6) and 81- (AS′1-AS′5) nt probes (Figs. 7A and 8A). As shown in Fig. 7B, antisense oligonucleotides AS2-AS5 prevented the protein binding to the 112-nt probe. Because the region covered by these oligonucleotides is the most CU-rich in the 3′UTR, the result suggests that a polypyrimidine-rich binding protein is involved in the complex formation. For the 81-nt probe, the AS′3 prevented the RNA-protein complex formation most efficiently, followed by the AS′4 (Fig. 8B). The AS′3 covers 16 nt of the 43-nt probe, which strongly binds the 70-kDa protein (Fig. 6B), and the rest of the AS′3 as well as the AS′4 cover parts of the 41-nt probe, which binds the protein less efficiently. This suggests that the binding site for the 70-kDa protein in the 3′UTR of iNOS mRNA probably is present within the sequence covered by AS′3 and AS′4, possibly involving the 16 nt at the 3′end of AS′3.

To test the affinities of the 60- and 70-kDa proteins for different nucleotides, competition assays with homoribopolymers and the 112- and 81-nt probes were performed. As shown in Fig. 9A, the binding to the 112-nt probe was efficiently inhibited by the poly(U) but not by the other homoribopolymers. This, together with experiments using antisense

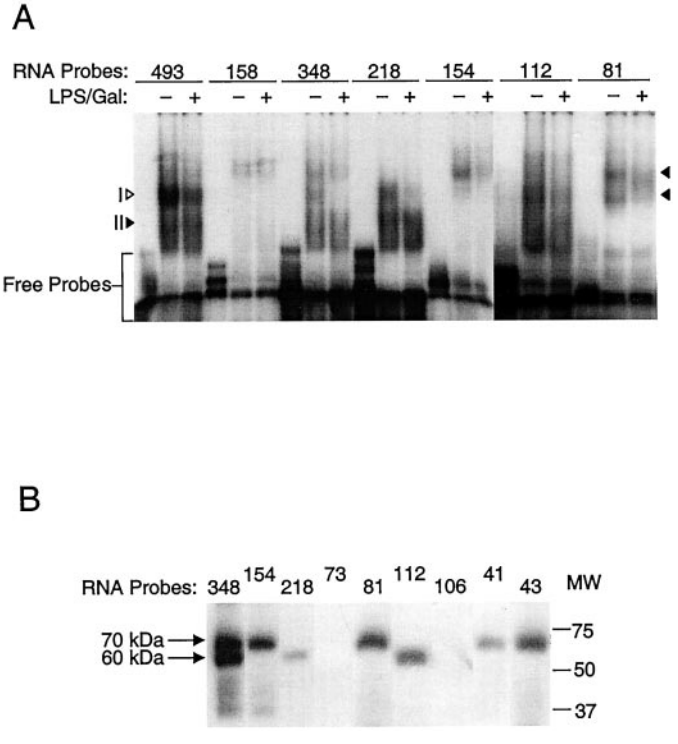

Fig. 6. Mapping of the protein binding sites. A, gel mobility shift assay with the 3′UTR 493-, 158-, 348-, 218-, 154-, 112-, and 81-nt RNA probes (see Fig. 2, Table 1) incubated with 5 μg of cytoplasmic protein extract from untreated (−) or "septic shock" (LPS/Gal) treated (+) mice. The first lane for each RNA probe contains no protein extract. The position of the free RNA probes and the RNA-protein complexes I (▷) and II (▶) are shown on the left. Closed arrows for the 81-nt complexes are indicated on the right. B, UV cross-linking with ^{32}P-radiolabeled 348-, 154-, 218-, 73-, 81-, 112-, 106-, 41-, and 43-nt RNA probes (see Fig. 2, Table 1) incubated with 25 μg of protein extract from untreated (−) or "septic shock" (LPS/Gal) treated (+) mice as described under *Materials and Methods*. Molecular mass (MW) standards in kilodaltons are indicated on the right, and the 70- and 60-kDa complexes are marked with arrows. Only proteins from untreated animals were used.

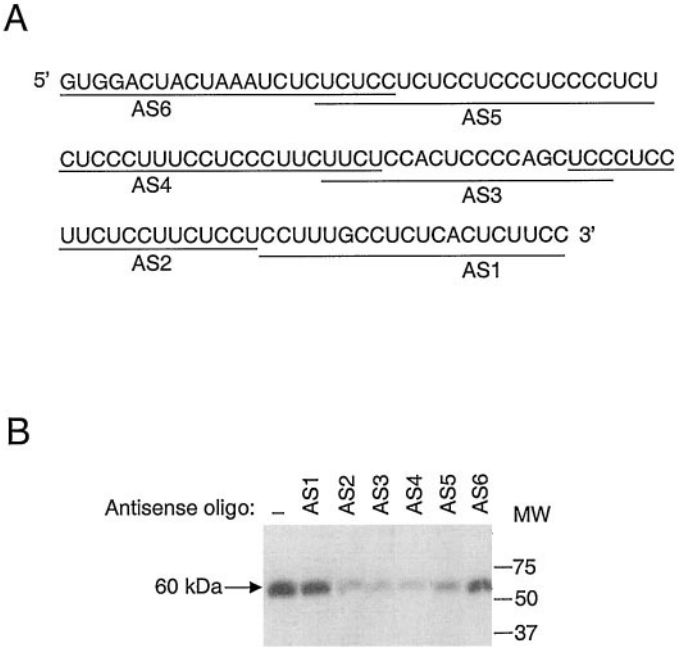

Fig. 7. Inhibition of the 60-kDa RNA-protein complex formation with antisense oligodeoxyribonucleotides. A, the iNOS 112-nt RNA sequence with the location of the 6 antisense (AS) oligodeoxyribonucleotides AS1 to AS6 is indicated. B, UV cross-linking analysis using 25 μg of cytoplasmic protein extract from untreated mice. The ^{32}P-radiolabeled 112-nt RNA probe was preincubated for 5 min in the absence (−) or presence of each of the six AS oligodeoxyribonucleotides (170 nM), as indicated, before addition of the protein extract. RNA-protein complexes were resolved on SDS/PAGE (12%). The 60-kDa complex is shown. Molecular mass (MW) standards in kilodaltons are indicated on the right.

oligoprobes, and the fact that the 112-nt sequence is extremely CU-rich (approximately 90% pyrimidines, Fig. 7A) suggest that the smaller, 60-kDa protein is a CU-rich binding protein. By contrast, none of the homoribopolymers prevented the complex formation with the 81-nt probe (Fig. 9B). Curiously, the poly(U) gave rise to a complex of higher molecular mass in addition to the 70-kDa complex. The observation that the 70 kDa protein does not interact with homoribopolymeric strands suggests that it recognizes a particular sequence at the 3′UTR (Fig. 9B).

A computer analysis (Mfold program) was performed to predict the secondary structure of the entire 3′UTR sequence (Fig. 10). It seems that in the most stable conformation, the high-affinity binding sites of both proteins lie within exposed areas, easily accessible for *trans*-acting factors. In addition, the tip of the loop including the binding site for the 70-kDa protein, is covered by the AS′3 oligonucleotide, which most efficiently prevented the binding in the competition assay (see Figs. 8 and 10).

Identification of the 60- and 70-kDa Proteins Binding to the 3′UTR of iNOS. Based on the characteristics of the smaller RNA-protein complex (an apparent molecular mass of 60 kDa, a high affinity for polyuridines, and a polypyrimidine-rich sequence), we postulated that this protein may be one form of the previously described hnRNP I/PTBs, 57- to 62-kDa multifunctional gene regulators (Hellen et al., 1993; Singh et al., 1995). To test this hypothesis, we performed immunoprecipitation of the UV cross-linked 112-nt RNA-protein complex. As shown in Fig. 11A, we were able to immunoprecipitate the 60-kDa complex with the anti-hnRNP I/PTB monoclonal antibody but not with the anti-hnRNP C or

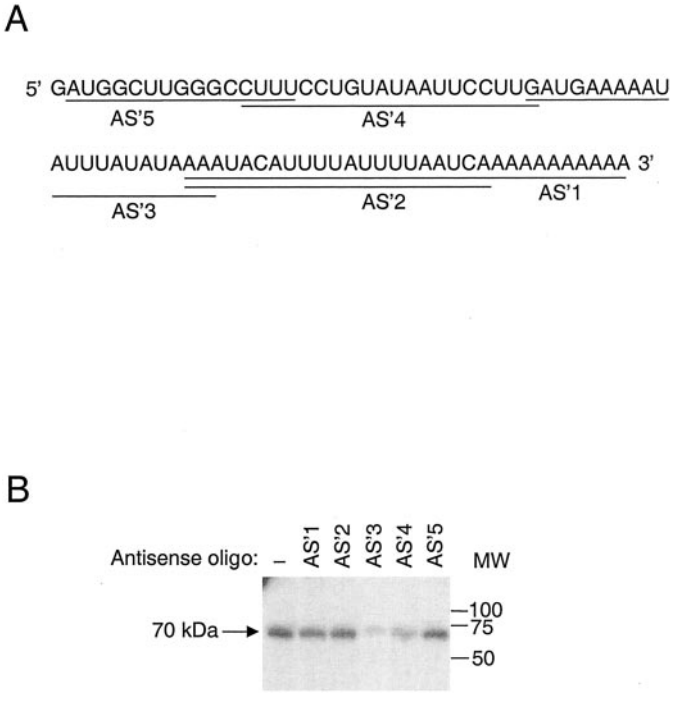

Fig. 8. Inhibition of the 70-kDa RNA-protein complex formation with antisense oligodeoxyribonucleotides. A, the iNOS 81-nt RNA sequence with the location of the five antisense (AS) oligodeoxyribonucleotides AS′1 to AS′5 is indicated. B, UV cross-linking analysis using 25 μg of cytoplasmic protein extract from untreated mice. The ^{32}P-radiolabeled 81-nt RNA probe was preincubated for 5 min in the absence (−) or presence of each of the five AS oligodeoxyribonucleotides (170 nM), as indicated, before addition of the protein extract. RNA-protein complexes were resolved on SDS/PAGE (12%). The 70-kDa complex is shown. Molecular mass (MW) standards in kilodaltons are indicated on the right.

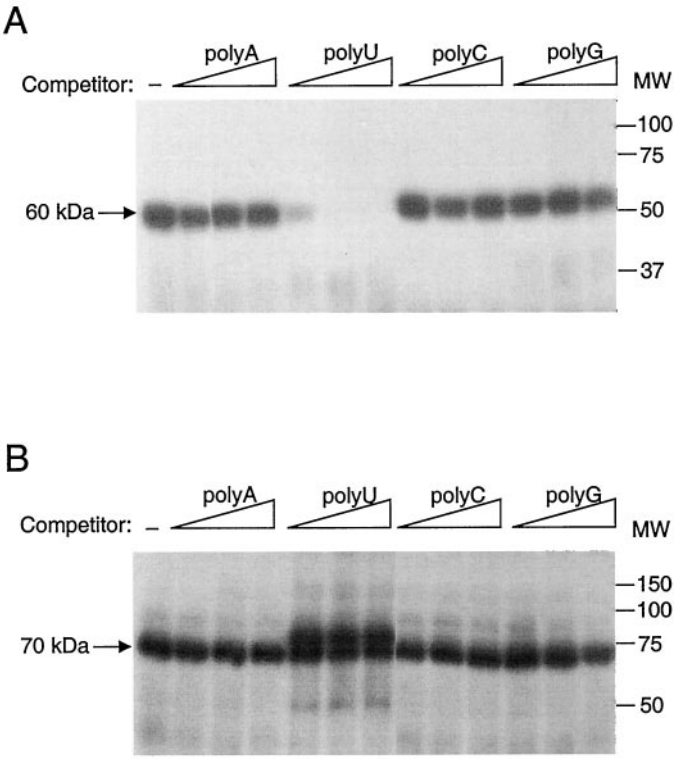

Fig. 9. Homoribopolymer affinity of the 60- and 70-kDa complexes. A, UV cross-linking competition assays were carried out with the ^{32}P-radiolabeled 112-nt fragment in the presence of 25 μg of cytoplasmic extract from untreated mice without (−) or with 10, 50, or 100 ng of unlabeled homoribopolymers poly(A), poly(U), poly(C), or poly(G), as indicated. Molecular mass (MW) standards in kilodaltons are indicated on the right. The 60-kDa complex is shown. B, UV cross-linking competition assays were carried out with the ^{32}P-radiolabeled 81-nt RNA probe in the presence of 25 μg of cytoplasmic extract from untreated mice without (−) or with 10, 50, or 100 ng of unlabeled homoribopolymers poly(A), poly(U), poly(C), or poly(G), as shown. Molecular mass (MW) standards in kilodaltons are indicated on the right. The 70-kDa complex is shown.

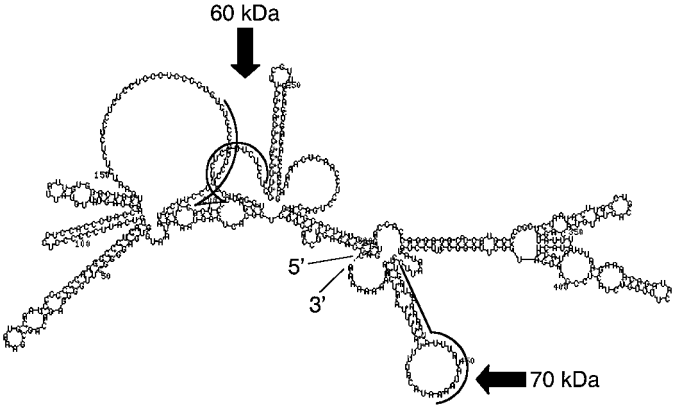

Fig. 10. Mfold computer predicted secondary structure of the 3′UTR of iNOS mRNA. The secondary structure of iNOS 3′UTR mRNA was predicted using the Mfold program (Mathews et al., 1999; Zuker et al., 1999). The structure in its most stable conformation is shown (minimum free energy dG = −109.7 kcal/mol). The putative binding sites for the proteins involved in the 60- and 70-kDa RNA-protein complexes, as defined by the covering of AS2–4 and AS′3, respectively, are indicated. Both are predicted to be situated in exposed loops, easily accessible for interactions with *trans*-acting factors.

hnRNP L antibodies, indicating that indeed this protein could be one of the variants of the hnRNP I/PTB.

Similarly, based on the apparent molecular mass of the 70-kDa complex and on previous observations on interactions between hnRNP I/PTB and hnRNP L (Hahm et al., 1998a), we postulated that this protein could be the hnRNP L. Immunoprecipitation of the UV cross-linked 81-nt RNA-protein complex, using the hnRNP L monoclonal antibody, demonstrates that the antibody recognizes the 70-kDa protein, although the band obtained is weak (Fig. 11B). Somewhat surprisingly, with the 81-nt probe, we also obtained the 60-kDa complex when using the anti-hnRNP I/PTB antibody. However, as seen in the overexposed UV cross-linked reference sample both bands are actually present, suggesting that both proteins are able to bind the 81-nt sequence.

Gel mobility shift assays with the full-length 493 iNOS 3′UTR probe and the anti-hnRNP I/PTB or anti-hnRNP L antibodies were then performed (Fig. 12). As a negative control we used the anti-hnRNP C antibody. A supershift could be shown only with the anti-hnRNP L antibody (Fig. 12).

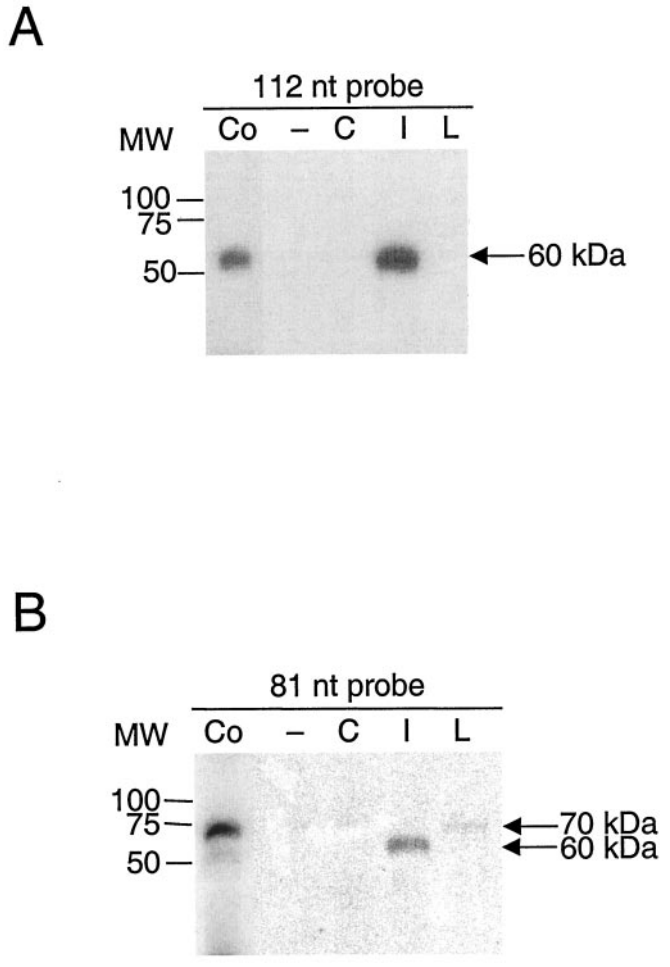

Fig. 11. Immunoprecipitation of the proteins in the 60- and 70-kDa RNA-protein complexes. A, UV cross-linking was performed with 200,000 cpm of ^{32}P-radiolabeled 112-nt RNA probe and 40 μg of liver cytoplasmic protein extract from untreated mice, followed by RNase A digestion. Immunoprecipitation was performed as described under *Materials and Methods*, without antibody (−) or with 1:500 dilution of the monoclonal antibodies anti-hnRNP C (C), anti-hnRNP I/PTB (I), or anti-hnRNP L (L), as indicated. A reference sample (UV cross-linking followed directly by SDS/PAGE) (Co) was included in the gel. The UV cross-linked lane was exposed on film for 2 days, whereas the immunoprecipitated samples were exposed for 1 week. Molecular mass (MW) standards in kilodaltons are indicated on the left. The 60-kDa complexes are marked with arrows. B, UV cross-linking was performed with 200,000 cpm of ^{32}P-radiolabeled 81-nt RNA probe and 40 μg of liver cytoplasmic protein extract from untreated mice, followed by RNase A digestion. Immunoprecipitation was performed as described under *Materials and Methods*, without antibody (−) or with 1:500 dilution of the monoclonal antibodies anti-hnRNP C (C), anti-hnRNP I/PTB (I), or anti-hnRNP L (L), as indicated. A reference sample (UV cross-linking followed directly by SDS/PAGE) (Co) was included in the gel. The UV cross-linked lane was exposed on film for 2 days, whereas the immunoprecipitated samples were exposed for 1 week and analyzed using autoradiographic imaging analysis. Molecular mass (MW) standards in kilodaltons are indicated on the left. The 60- and 70-kDa complexes are marked with arrows.

Discussion

Several lines of evidence suggest that post-transcriptional events are important in the regulation of the iNOS expression, but only little is known of their molecular mechanisms (Vodovotz et al., 1993; Weisz et al., 1994; Rodriguez-Pascual et al., 2000). In this study, we identified two liver cytoplasmic proteins of 60 and 70 kDa, interacting with the 3′UTR of the murine iNOS mRNA, and our evidence strongly indicates that these proteins are hnRNP I/PTB and hnRNP L, respectively. Their binding to the 3′UTR of the mRNA is affected by septic shock, which suggests a role in the post-transcriptional events of iNOS induction by inflammation.

The RNA binding characteristics of the 60-kDa protein indicates that it may be one variant of the hnRNP I/PTB (Hellen et al., 1993; Singh et al, 1995). Its binding site at the iNOS mRNA is a polypyrimidine-rich sequence, showing a high nucleotide identity with known PTB consensus sequences (Singh et al., 1995): the 112-nt sequence at the iNOS 3′UTR, containing the high-affinity binding site, includes a 15-nt stretch in the 5′ end with 87% identity to the known PTB consensus sequence. In addition, a region in the middle

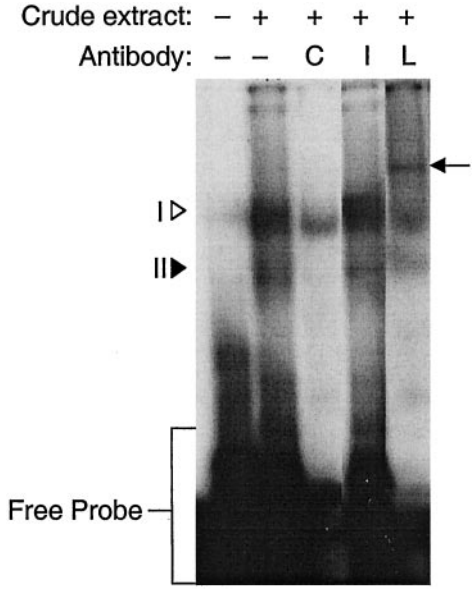

Fig. 12. Antibody supershift of the gel shift complex. The ^{32}P-radiolabeled 3′UTR 493-nt probe incubated in the absence (−) or in the presence (+) of 5 μg of cytoplasmic protein extract as described for the gel mobility shift assay, was incubated without (−) or with 1 μl of the monoclonal antibodies anti-hnRNP C (C), anti-hnRNP I/PTB (I), or anti-hnRNP L (L), as indicated. Samples (10 μl) were loaded on the gel. The positions of the complexes I (▷) and II (▶) are indicated. The supershifted complex is marked on the right. The position of the free RNA probe is shown.

of the 112-nt sequence show 77% identity with a 26-nt sequence in GAP-43 3′UTR mRNA, which has been reported to bind a PTB-like protein (Irwin et al., 1997). Another sequence, similar to the known hnRNP I/PTB binding sites, is found 42 nt upstream of the possible hnRNP L binding site in the iNOS 3′UTR. This may explain why the 60-kDa protein was found to interact at two distinct regions of the 3′UTR (Figs. 8 and 11B).

Similarly, the size of the other protein (70 kDa) binding to iNOS 3′UTR and the 70% nt identity of its binding site at the iNOS mRNA with a known binding site of hnRNP L in vascular endothelial growth factor 3′UTR mRNA, led us to hypothesize that this protein is the hnRNP L (Shih and Claffey, 1999).

Immunoprecipitation of the UV cross-linked complexes and supershift of the native complex confirmed that the two proteins binding to the 3′UTR of the iNOS mRNA are the hnRNP I/PTB and hnRNP L or highly similar proteins. The absence of strict consensus binding sequences in the different mRNA target molecules described in the literature suggests that the proteins have some flexibility in their RNA sequence recognition. Such flexibility has been shown for the hnRNP A1 (Burd and Dreyfuss, 1994). Alternatively, the two proteins described here could be close structural analogs of the hnRNP I/PTB and L species described previously, with modified RNA binding characteristics. This is possible, particularly in the case of hnRNP I/PTB, for which several variants have been described previously (Gil et al., 1991; Markovtsov et al., 2000).

Previous studies have shown that hnRNP I/PTB interacts with hnRNP L (Hahm et al., 1998a). Our studies are in agreement with the previous observations, although they do not reveal the exact nature of the interaction. When the major complex appearing in the gel-shift assay is UV cross-linked and resolved by SDS/PAGE, two bands of approximately 60 and 70 kDa are detected, showing that both proteins are present in the native complex (data not shown). Furthermore, the poly(U) homoribopolymer efficiently prevented the formation of the entire gel shifted complex (data not shown). Yet, of the two proteins described here, only the 60-kDa protein binding to the 3′UTR was poly(U) sensitive, thus suggesting that this protein is critical for the multiprotein complex formation. Also, the lack of native complex formation with the 81-nt probe, which contains the binding site for the hnRNP L, and where the hnRNP I/PTB seems to interact only weakly, suggests that the high-affinity binding of hnRNP I/PTB with the RNA is prerequisite for the binding of hnRNP L in the native complex. It is therefore interesting to note that only the anti-hnRNP L antibody caused a supershift of the native complex. This could indicate that whereas the hnRNP I/PTB regulates the interaction of the entire complex with the RNA, the hnRNP L is more exposed at the surface of the multiprotein complex.

So far, only one *trans*-acting factor has been described interacting with the 3′UTR of iNOS mRNA: Rodriguez-Pascual et al. (2000) have shown that the HuR protein interacts with AUUUA rich sequences of the iNOS mRNA in human DLD-1 cells and hypothesize that the protein may take part in mRNA stabilization. We did not find any evidence for the binding of HuR to mouse iNOS mRNA, and neither of the two proteins described here had affinity for AUUUA motifs (data not shown). An explanation for these essentially different results could be that *trans*-acting factors interacting with iNOS mRNA can be cell- and species-specific.

The hnRNP I/PTB seems to be involved in several processes, such as alternative splicing (Singh et al., 1995), viral replication (Chung and Kaplan, 1999), alteration of RNA conformation (Huang and Lai, 1999) and cap-independent translation through internal ribosomal entry sites (Hellen et al., 1993). The protein has been shown to shuttle between the cytoplasm and the nucleus in a transcription-linked manner (Michael et al., 1995), suggesting distinct roles in the different subcellular compartments. Irwin et al. (1997) propose that the interaction of hnRNP I/PTB with the 3′UTR of the bovine brain GAP-43 mRNA could stabilize the transcript and Kim et al. (2000b) show that the hnRNP I/PTB inhibits translation of Bip (an immunoglobulin heavy-chain binding protein) dependent on internal ribosomal entry sites.

The hnRNP L is highly homologous to hnRNP I (Piñol-Roma et al., 1989) and is also found to shuttle between the nucleus and the cytoplasm in a transcription-dependent manner (Michael et al., 1995; Hahm et al., 1998b). Several functions have been assigned to hnRNP L: e.g., modulation of the human vascular endothelial growth factor labile mRNA stability under hypoxic conditions (Shih and Claffey, 1999) and the translation of hepatitis C virus mRNA (Hahm et al., 1998b).

Both hnRNP I/PTB and hnRNP L contain four loosely conserved RNA recognition motifs, and it has been shown that they may form homodimers and/or heterodimers with other hnRNPs [e.g., the hnRNP E2, I, K and L (Kim et al., 2000a)]. It has therefore been suggested that some of their effects are exerted in concert (Hahm et al., 1998a). Potential roles of the heterodimer on RNA processing, mRNA nucleocytoplasmic transport and/or translation of some mRNAs have been proposed. It is also possible that the hnRNP I/PTB-hnRNP L complex has an RNA-binding specificity different from the individual proteins and thus exert a different function compared with the individual proteins (Hahm et al., 1998a).

In conclusion, we describe for the first time the interaction of hnRNP I/PTB and hnRNP L with the murine iNOS mRNA and the modulation of this interaction by inflammation, a strong inducer of the iNOS expression. The modulated interaction with the iNOS mRNA suggests a novel function for hnRNP I/PTB and hnRNP L. We do not know how septic shock affects the affinity of the proteins for the iNOS mRNA, but, based on their previously described functions, we can speculate on their possible roles in the iNOS induction. The hnRNP I/PTB could inhibit translation during resting conditions alone, as shown in the case of the Bip mRNA (Kim et al., 2000b), or concertedly with hnRNP L (Kim et al., 2000a). Alternatively, the two proteins may participate in the rapid iNOS mRNA degradation under noninduced conditions. Indeed, we detect a strong RNA-protein complex in resting cells where the iNOS transcripts are hardly detectable, even though significant transcription of the *iNOS* gene is going on (de Vera et al., 1996; Linn et al. 1997; Rodriguez-Pascual, 2000). The discrepancy between the high transcription level and low amounts of iNOS mRNA in resting cells can be explained by an efficient degradation of the iNOS transcript (Rodriguez-Pascual et al., 2000). In inflammation, this could be reversed, resulting in stimulation of gene expression (at least in part) via an increase in mRNA stability. How the inflammation-modulated binding of hnRNP I/PTB and

hnRNP L to the iNOS mRNA relates to the mRNA stability and other post-transcriptional events is a focal point of our future research.

Acknowledgments

We are grateful to Dr. Charles J. Lowenstein for providing the murine iNOS cDNA plasmid and to Dr. Gideon Dreyfuss for supplying the anti-hnRNP C and anti-hnRNP L antibodies. We also thank Kyle Christian for careful reading of the manuscript.

References

Barton BE and Jackson JV (1993) Protective role of interleukin 6 in the lipopolysaccharide-galactosamine septic shock model. *Infect Immun* **61:**1469–1499.

Burd CG and Dreyfuss G (1994) RNA binding specificity of hnRNP A1: significance of hnRNP A1 high-affinity binding sites in pre-mRNA splicing. *EMBO (Eur Mol Biol Organ) J* **13:**1197–1204.

Chu SC, Marks-Konczalik J, Wu H-P, Banks TC, and Moss J (1998) Analysis of the cytokine-stimulated human inducible nitric oxide synthase (iNOS) gene: characterization of differences between human and mouse iNOS promoters. *Biochem Biophys Res Commun* **248:**871–878.

Chung RT and Kaplan LM (1999) Heterogeneous nuclear ribonucleoprotein I (hnRNP-I/PTB) selectively binds the conserved 3′ terminus of hepatitis C viral RNA. *Biochem Biophys Res Commun* **254:**351–362.

Church GM and Gilbert W (1984) Genomic sequencing. *Proc Natl Acad Sci USA* **81:**1991–1995.

Corbett JA and McDaniel ML (1992) Does nitric oxide mediate autoimmune destruction of β-cells? Possible therapeutic interventions in IDDM. *Diabetes* **41:**897–903.

Cui S, Reichner JS, Mateo RB, and Albina JE (1994) Activated murine macrophages induce apoptosis in tumor cells through nitric oxide-dependent or -independent mechanisms. *Cancer Res* **54:**2462–2467.

de Vera ME, Shapiro RA, Nussler AK, Mudgett JS, Simmons RL, Morris SM, Billiar TR, and Geller DA (1996) Transcriptional regulation of human inducible nitric oxide synthase (NOS2) gene by cytokines: initial analysis of the human NOS2 promoter. *Proc Natl Acad Sci USA* **93:**1054–1059.

Evans T, Carpenter A, and Cohen J (1994) Inducible nitric-oxide-synthase mRNA is transiently expressed and destroyed by a cycloheximide-sensitive process. *Eur J Biochem* **219:**563–569.

Geller DA and Billiar TR (1998) Molecular biology of nitric oxide synthases. *Cancer Metastasis Rev* **17:**7–23.

Gil A, Sharp PA, Jamison SF, and Garcia-Blanco MA (1991) Characterization of cDNAs encoding the polypyrimidine tract-binding protein. *Genes Dev* **5:**1224–1236.

Hahm B, Cho OH, Kim J-E, Kim YK, Kim JH, Oh YL, and Jang SK (1998a) Polypyrimidine tract-binding protein interacts with hnRNP L. *FEBS Lett* **425:**401–406.

Hahm B, Kim YK, Kim JH, Kim TY, and Jang SK (1998b) Heterogeneous nuclear ribonucleoprotein L interacts with the 3′ border of the internal ribosomal entry site of hepatitis C virus. *J Virol* **72:**8782–8788.

Hamilton BJ, Nagy E, Malter JS, Arrick BA, and Rigby WFC (1993) Association of heterogeneous nuclear ribonucleoprotein A1 and C proteins with reiterated AUUUA sequences. *J Biol Chem* **268:**8881–8887.

Hellen CUT, Witherell GW, Schmid M, Shin SH, Pestova TV, Gil A, and Wimmer E (1993) A cytoplasmic 57-kDa protein that is required for translation of picornavirus RNA by internal ribosomal entry is identical to the nuclear pyrimidine tract-binding protein. *Proc Natl Acad Sci USA* **90:**7642–7646.

Huang P and Lai MMC (1999) Polypyrimidine tract-binding protein binds to the complementary strand of the mouse hepatitis virus 3′untranslated region, thereby altering RNA conformation. *J Virol* **73:**9110–9116.

Irwin N, Baekelandt V, Goritchenko L, and Benowitz LI (1997) Identification of two proteins that bind to a pyrimidine-rich sequence in the 3′-untranslated region of GAP-43 mRNA. *Nucleic Acids Res* **25:**1281–1288.

Kim JH, Hahm B, Kim YK, Choi M, and Jang SK (2000a) Protein-protein interaction among hnRNPs shuttling between nucleus and cytoplasm. *J Mol Biol* **298:**395–405.

Kim YK, Hahm B, and Jang SK (2000b) Polypyrimidine tract-binding protein inhibits translation of Bip mRNA. *J Mol Biol* **304:**119–133.

Linn SC, Morelli PJ, Edry I, Cottongim SE, Szabo C, and Salzman AL (1997) Transcriptional regulation of human inducible nitric oxide synthase gene in an intestinal epithelial cell line. *Am J Physiol* **272:**G1499–G1508.

Lowenstein CJ, Alley EW, Raval P, Snowman AM, Snyder SH, Russel SW, and Murphy WJ (1993) Macrophage nitric oxide synthase gene: two upstream regions mediate induction by interferon-γ and lipopolysaccharide. *Proc Natl Acad Sci USA* **90:**9730–9734.

Lowenstein CJ, Glatt CS, Bredt DS, and Snyder SH (1992) Cloned and expressed macrophage nitric oxide synthase contrasts with the brain enzyme. *Proc Natl Acad Sci USA* **89:**6711–6715.

Lowry OH, Rosebrough NJ, Farr AL, and Randall RJ (1951) Protein measurement with the folin phenol reagent. *J Biol Chem* **193:**265–275.

Markovtsov V, Nikolic JM, Goldman JA, Turck CW, Chou M-Y, and Black DL (2000) Cooperative assembly of an hnRNP complex induced by a tissue-specific homolog of polypyrimidine tract binding protein. *Mol Cell Biol* **20:**7463–7479.

Mathews DH, Sabina J, Zuker M, and Turner DH (1999) Expanded sequence dependence of thermodynamic parameters improves prediction of RNA secondary structure. *J Mol Biol* **288:**911–940.

McCartney-Francis N, Allen JB, Mizel DE, Albina JE, Xie Q, Nathan CF, and Wahl SM (1993) Suppression of arthritis by an inhibitor of nitric oxide synthase. *J Exp Med* **178:**749–754.

Michael WM, Siomi H, Choi M, Piñol-Roma S, Nakielny S, Liu Q, and Dreyfuss G (1995) Signal sequences that target nuclear import and nuclear export of pre-mRNA-binding proteins. *Cold Spring Harb Symp Quant Biol* **60:**663–668.

Min H, Chan RC, and Black DL (1995) The generally expressed hnRNP F is involved in a neural-specific pre-mRNA splicing event. *Genes Dev* **9:**2659–2671.

Morikawa A, Kato Y, Sugiyama T, Koide N, Chakravortty D, Yoshida T, and Yokochi T (1999) Role of nitric oxide in lipopolysaccharide-induced hepatic injury in D-galactosamine-sensitized mice as an experimental endotoxic shock model. *Infect Immun* **67:**1018–1024.

Nathan CF and Hibbs JB Jr (1991) Role of nitric oxide synthesis in macrophage antimicrobial activity. *Curr Opin Immunol* **3:**65–70.

Piñol-Roma S, Swanson MS, Gall JG, and Dreyfuss G (1989) A novel heterogeneous nuclear RNP protein with a unique distribution on nascent transcripts. *J Cell Biol* **109:**2575–2587.

Rao MK (2000) Molecular mechanisms regulating iNOS expression in various cell types. *J Toxicol Environ Health B Crit Rev* **3:**27–58.

Rodriguez-Pascual F, Hausding M, Ihrig-Biedert I, Furneaux H, Levy AP, Förstermann U, and Kleinert H (2000) Complex contribution of the 3′untranslated region to the expressional regulation of the human inducible nitric-oxide synthase gene—involvement of the RNA-binding protein HuR. *J Biol Chem* **275:**26040–26049.

Ross J (1995) mRNA stability in mammalian cells. *Microbiol Rev* **59:**423–450.

Shih S-C and Claffey KP (1999) Regulation of human vascular endothelial growth factor mRNA stability in hypoxia by heterogeneous nuclear ribonucleoprotein L. *J Biol Chem* **274:**1359–1365.

Singh R, Valcárcel J, and Green MR (1995) Distinct binding specificities and functions of higher eukaryotic polypyrimidine tract-binding proteins. *Science (Wash DC)* **268:**1173–1176.

Vodovotz Y, Bogdan C, Paik J, Xie Q, and Nathan C (1993) Mechanisms of suppression of macrophage nitric oxide release by transforming growth factor β. *J Exp Med* **178:**605–613.

Weisz A, Oguchi S, Cicatiello L, and Esumi H (1994) Dual mechanism for the control of inducible-type NO synthase gene expression in macrophages during activation by interferon-γ and bacterial lipopolysaccharide. Transcriptional and post-transcriptional regulation. *J Biol Chem* **269:**8324–8333.

Xie Q, Whisnant R, and Nathan C (1993) Promoter of the mouse gene encoding calcium-independent nitric oxide synthase confers inducibility by interferon γ and bacterial lipopolysaccharide. *J Exp Med* **177:**1779–1784.

Zuker M, Mathews DH, and Turner DH (1999) Algorithms and thermodynamics for RNA secondary structure prediction: a practical guide, in *RNA Biochemistry and Biotechnology* (Barciszewski J and Clark BFC eds) pp 11–43, NATO ASI Series, Kluwer Academic Publishers, Netherlands.

Address correspondence to: Dr. Malin Söderberg, Division of Biochemistry, Department of Pharmaceutical Biosciences, Box 578 Biomedicum, SE-751 23 Uppsala, Sweden. E-mail: malin.hobro-soderberg@farmbio.uu.se